Articles

Novel *Seco*ergoline Derivatives Inhibit Both GABA and Glutamate Uptake in Rat Brain Homogenates: Synthesis, in Vitro Pharmacology, and Modeling

László Héja,[†] Ilona Kovács,[†] Éva Szárics,[†] Mária Incze,[‡] Eszter Temesváriné-Major,[‡] Gábor Dörnyei,[‡] Mária Peredy-Kajtár,[§] Eszter Gács-Baitz,[§] Csaba Szántay,[‡] and Julianna Kardos*[,†]

Department of Neurochemistry, Department of Natural Organic Compounds, and NMR Laboratory, Chemical Research Center, Hungarian Academy of Sciences, H-1025 Pusztaszeri út 59-67, Organic Chemistry Institute, Budapest University of Technology and Economics, H-1111 Gellért tér 4, Budapest, Hungary

Received March 12, 2004

Three of twelve secoergoline derivatives (*Z* ethyl 4-[(ethoxycarbonylmethyl)methylamino]-2-methyl-3-phenylpent-2-enoate, **8**; ethyl 1,6-dimethyl-3-oxo-5-phenyl-1,2,3,6-tetrahydropyridine-2-carboxylate, **9**; *Z* methyl 4-[(methoxycarbonylmethyl)methylamino)-2-methyl-3-phenylpent-2-enoate, **11**), containing bioisosteric sequences of GABA and Glu, inhibited both GABA and Glu transport through cerebrocortical membranes specifically. Compounds **8**, **9**, and **11** appeared to be equipotent inhibitors of GABA and Glu transport with IC_{50} values between 270 and 1100 μM, whereas derivatives **1**−**7**, **10**, and **12** were without effects. In the presence of GABA and Glu transport-specific nontransportable inhibitors, inhibition of GABA and Glu transport by **8**, **9**, and **11** proceeded in two phases. The two phases of inhibition were characterized by IC_{50} values between 4 and 180 nM and 360−1020 μM and different selectivity sequences**.** These findings may indicate the existence of some mechanism possibly mediated by a previously unrecognized GABA-Glu transporter. Derivatives with the cis, but not the trans configuration of bulky ester groups (**8** vs **7** and **11** vs **12**) showed significant inhibitory effect (IC_{50} values of 270 μM vs ≫1000 μM and 1100 μM vs ≫1000 μM on GABA transport, respectively). The *cis*−*trans* selectivity can be explained by docking these *seco*ergolines in a three-dimensional model of the second and third transmembrane helices of GABA transporter type 1.

Introduction

Epilepsy, one of the most common neurological disorder, which affects ∼1−2% of the population worldwide,[1] may be controlled by both the facilitation of γ-aminobutyric acid (GABA)-mediated (GABA*ergic*) inhibitory pathways[2] and the inhibition of glutamic acid-mediated (Glu*ergic*) excitatory neurotransmission.[3] Although there is evidence that Glu*ergic* excitatory neurotransmission may contribute to the pathophysiology of epilepsy, development of novel *N*-methyl-D-aspartate (NMDA) receptor antagonists as antiepileptic drugs has been terminated because of their low efficiency and wide-range side effects in clinical trials.[4] Development of α-amino-3-hydroxy-5-methyl-4-isoxazolepropionic acid (AMPA) receptor antagonists may have a role for the control of symptoms. Indeed, suppression of seizures in a low-[Mg^{2+}] ion model of experimental epilepsy was observed with the use of a quinazolone-alkyl-carboxylic acid derivative,[5] known to block (*S*)(+)AMPA-induced transmembrane Ca^{2+} ion influx.[6]

Among the rational strategies, the most widely used way to develop new antiepileptic drugs is based on the GABA hypothesis of epilepsy.[7] Accordingly, impairment of GABA*ergic* pathways is of deciding importance for the pathogenesis of several types of epilepsy. Thus, the GABA approach to antiepileptic therapy can be directed at the development of novel GABA- and benzodiazepine-mimetic derivatives targeting $GABA_A$ receptors as well as GABA uptake inhibitors as potential drugs for epilepsy.[7−9] It is of note in this context that the residues which form a salt bridge between the gamma and beta subunits of $GABA_A$ receptors have been implicated in epilepsy-inducing mutations.[10] Despite advances, our understanding of how neurotransmitter transporters work is limited by a lack of three-dimensional structural information.[11]

In the absence of high-resolution structural data, computer-aided predictions of the three-dimensional structure of GABA transporter type 1 (GAT1), the prototypical member of a group of proteins with a GABA transport role in the vertebrate central nervous system, together with the localization of amino acid residues crucial for GABA recognition[12,13] can be explored. Based on these studies and pharmacological data for a series of known GABA transport inhibitors, and using the transmembrane helix 3 and transmembrane helix 2 (TM3 and TM2) regions of GAT1, a model of the three-dimensional structure of the ligand binding crevice in the GAT1 transporter has been developed. We report here the synthesis and pharmacological characterization

* To whom correspondence should be addressed. Tel.: +36 1 325 9101; fax: +36 1 325 7554; e-mail: jkardos@chemres.hu.
[†] Department of Neurochemistry.
[‡] Department of Natural Organic Compounds.
[§] NMR Laboratory.

10.1021/jm040809c CCC: $27.50
Published on Web 10/05/2004

Scheme 1. Synthetic Routes to **1**−**4**

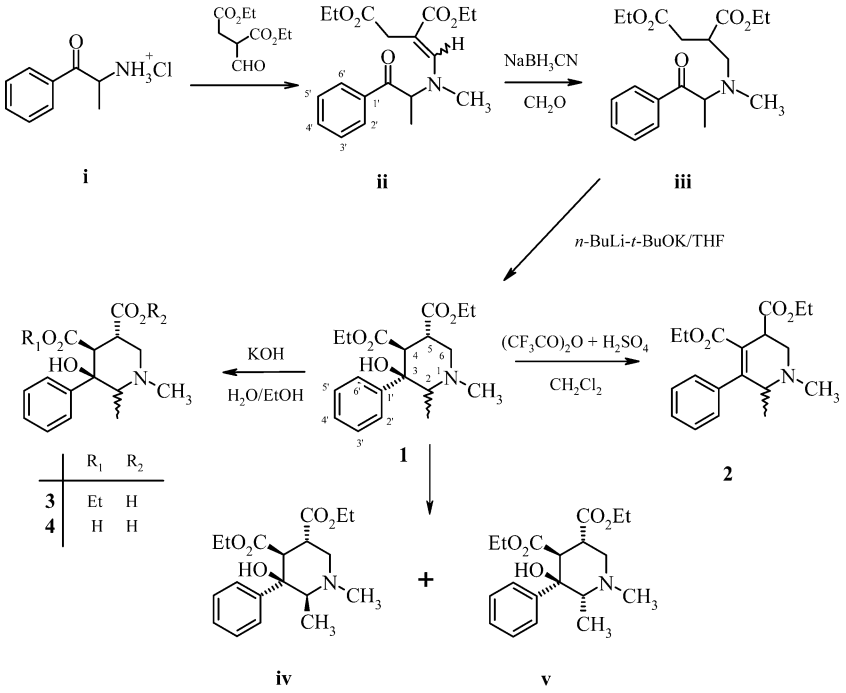

Scheme 2. Synthetic Routes to **5**−**12**

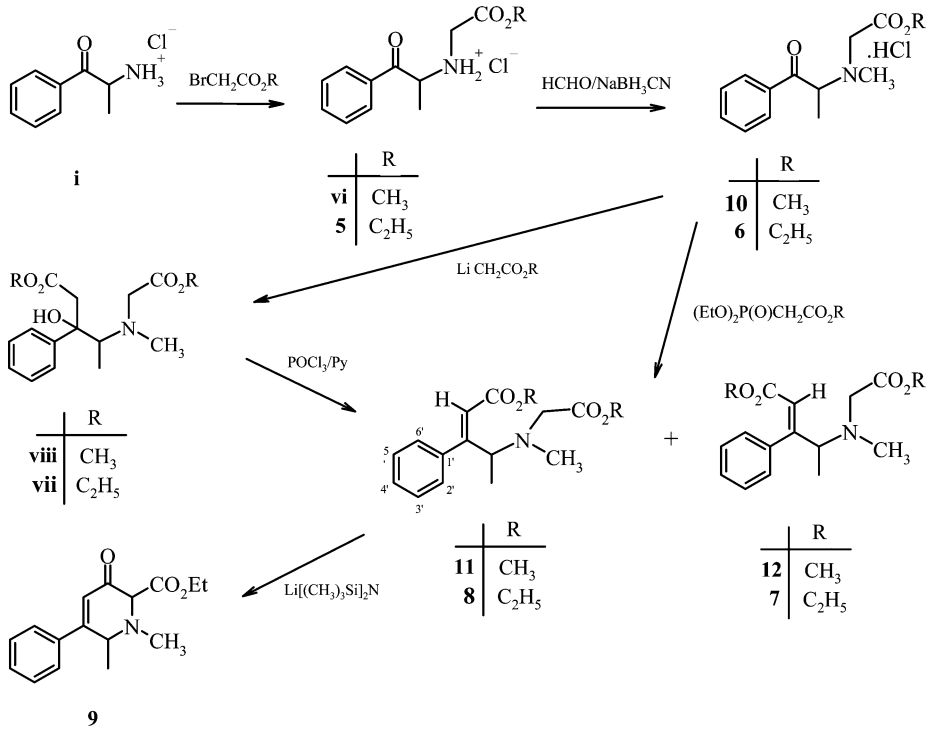

of new *seco*ergoline derivatives. The results of docking to the model have enabled us to rationalize the observed efficiency and selectivity of **7** and **8**.

Results

Chemistry. All the chiral compounds are racemates; however, they are represented by drawing only one of the enantiomers in the schemes. The tested compounds (indicated by Arabic numbers) were synthesized starting from 1-phenyl-2-aminopropan-1-one hydrochloride (**i**) as shown in Schemes 1 and 2. To prepare compounds **1**−**4** (Scheme 1), α-aminoketone (**i**), obtained from propiophenone according to Bennett et al.[14] and House et al.,[15] was treated with diethyl α-formylsuccinate according to a method described by Stoll et al.[16] The double bond of the geometric isomers of enamines **ii** thus obtained was reduced, and a parallel reductive methylation with formaldehyde and $NaBH_3CN$ furnished diester **iii**. Stobbe-type ring closure of the latter to piperidine derivative **1** was performed with super base BuLi+tBuOK in tetrahydrofuran (THF). **1** is a diastereomic mixture of **iv** and **v**, which could be separated either by fractionated crystallization or by column chromatography. Water elimination from **1** to

Table 1. IC_{50} Values of *Seco*ergoline Derivatives on Specific [^{3}H]GABA and [^{3}H]DASP Transport through Cerebrocortical Membranes at 30 °C. Number of Experiments: $N = 2$ to $N = 6$

	IC_{50} (μM)	
compound	[^{3}H]GABA transport	[^{3}H]DASP transport
1	≫1000	≫1000
2	≫1000	≫1000
3	≫1000	≫1000
4	≫1000	≫1000
5	≫1000	≫1000
6	≫1000	≫1000
7	≫1000	≫1000
8	270 ± 43	420 ± 57
9	680 ± 87	660 ± 61
10	≫1000	≫1000
11	1100 ± 128	1100 ± 105
12	≫1000	≫1000

give **2** was accomplished by treatment with trifluoroacetic anhydride, both this and the previous steps according to Moldvai et al.[17] Aqueous KOH hydrolysis of **1** at 60 °C (3 h) gave a ca. 2:1 mixture of half ester **3** and dicarboxylic acid **4**. Separation of the two compounds was performed by column chromatography. To synthesize compounds **5**−**12** (Scheme 2), α-aminoketone (**i**) was first alkylated with ethyl and methyl bromoacetate to produce **5** and **vi**, reductive methylation of which gave tertiary amines **6** and **10**, respectively. β-Hydroxy esters **vii** and **viii** were prepared according to Rathke's method[18] by reacting the keto function with lithio acetates generated in situ with lithium bis(trimethylsilyl)amide at −78 °C. Water elimination from these hydroxy compounds was performed with $POCl_3$/pyridine according to the method of Mehta et al.[19] The two geometric isomer pairs **7**, **8** and **11**, **12** were prepared in another way as well, via phosphonate condensation of ketones **6** and **10** according to the method described by Wadworth et al.[20] The isomers were separated by column chromatography, and the geometry of the double bond was elucidated by NOE measurements. Strong interaction between the olefinic proton and 2′ and 6′ aromatic protons verifies the *Z* geometry in **8** and **11**, and that with all of the CH_3CHNCH_3 protons verifies the *E* geometry in **7** and **12** (see Experimental Section). Finally Dieckmann-condensation of isomer *Z* of ethyl ester **8** in THF with lithium bis(trimethylsilyl)amide as base at room temperature gave piperidone derivative **9**. As seen by NMR measurements, piperidone derivative **9** equilibrates with the H-bond containing enol tautomer in solution. For receptor binding and uptake investigations, all the compounds were transformed into water-soluble hydrochloride salts.

In Vitro Pharmacology. Effects of *seco*ergoline derivatives on GABA and Glu transport through cerebrocortical membranes are summarized in Table 1. To verify test conditions, the IC_{50} value of a specific GABA uptake inhibitor, 1,2,5,6-tetrahydropiridine-3-carboxylic acid (guvacine), has been determined. It was found to be 6.25 ± 0.86 μM after 10 min preincubation with guvacine. This value compares with data in the literature (8.7 ± 0.2 μM, no preincubation;[21] 4.92 ± 1.02 μM, 15 min preincubation[22]). Also in agreement with the literature, the IC_{50} value of a specific Glu uptake inhibitor, l-*trans*-pyrrolidine-2,4-dicarboxylic acid (t-PDC) was found to be 5.64 ± 0.85 μM (5.1 ± 0.3[23]). *Seco*ergoline derivatives with the cis, but not the trans, configuration of bulky ester groups (**8** vs **7** and **11** vs **12**) showed significant inhibitory effect. The *seco*ergoline derivatives **8**, **9**, and **11** gave IC_{50} values of 270 ± 43, 680 ± 87 and 1100 ± 128 μM on GABA uptake, respectively. Surprisingly, **8**, **9**, and **11** showed similar inhibitory potential on Glu transport with IC_{50} values of 420 ± 57, 660 ± 61, and 1100 ± 105 μM, respectively (Table 1). *Seco*ergoline derivatives found to be ineffective on GABA uptake did not show any significant effect on Glu transport, either (Table 1).

Measurements on the effects of **8**, **9**, and **11** on GABA uptake were performed in the presence of 100 μM 1,2,5,6-tetrahydro-1-[2-[[(diphenylmethylene)amino]oxy]-ethyl]-3-pyridine carboxylic acid hydrochloride (NNC-711) (Table 2), a potent, specific, nontransportable inhibitor of GAT1.[24] In this case, the dose−response curves showed two phases, indicating the presence of two separate GABA transport processes (Figure 1). In one of these phases **8**, **9**, and **11** gave IC_{50} values comparable, but not equal to those obtained in the absence of NNC-711 (380 ± 13, 360 ± 8, and 491 ± 14 μM, respectively), whereas IC_{50} values obtained for **8**, **9**, and **11** in the other phase were found to be 180 ± 7, 3.7 ± 0.6, and 44 ± 2 nM, respectively. In addition, effects of **8**, **9**, and **11** on Glu transport were determined in the presence of 100 μM DL-*threo*-β-benzyloxyaspartic acid (DL-TBOA) (Table 2), a potent, nontransportable inhibitor of Glu transporter types 1−5.[25] As seen with GABA transport by the presence of NNC-711, the dose−response curves also showed two phases suggesting that **8**, **9**, and **11** act on two separate Glu transport processes (Figure 1). In one of the phases **8**, **9**, and **11** gave IC_{50} values similar to those obtained in the absence of DL-TBOA (385 ± 16, 591 ± 24, and 1019 ± 81 μM, respectively), whereas the other phase was characterized by IC_{50} values of 34 ± 2, 9.0 ± 0.2, and 11 ± 0.9 nM, respectively.

Specificity of *seco*ergoline derivatives as uptake inhibitors was addressed in measurements of $GABA_A$, $GABA_B$, AMPA, NMDA, and (2*S*,3*S*,4*R*)-carboxy-4-(1-methylethenyl)-3-pyrrolidineacetic acid (kainate) receptor binding. Neither of *seco*ergoline derivatives in 10 μM ($GABA_A$), 100 μM ($GABA_B$), and 30 μM (AMPA, NMDA, kainate) inhibited the binding of labeled specific ligands to these receptors significantly (data not shown).

Molecular Modeling. The One-TM Model. To find amino acid residues possibly involved in binding, the nonflexible GABA transport inhibitor, guvacine, was docked in the model of the TM3 region of GAT1. H-Bonding interactions were found between functional groups of residues, Tyr-140(OH), Asn-137(C=O), Ser-133(OH), and guvacine (C=O, OH, NH, respectively). In this way, all polar amino acids of GAT1 TM3 participated in H-bonding interactions except Tyr-139, which is faced perpendicularly to Tyr-140. It is to note in this respect, that Tyr-139 was found unnecessary for ligand binding.[13] To verify binding calculations obtained by docking guvacine in the model of GAT1 TM3, known inhibitors, such as GABA, (*R*)(−)-*N*-(4,4-di-(3-methylthien-2-yl)but-3-enyl)nipecotic acid hydrochloride (tiagabine), and the (*R*)(−) and (*S*)(+) isomers of 3-piperidinecarboxylic acid ((*R*) and (*S*)nipecotic acid) were docked in the model of GAT1 TM3, in addition to cis (**8**) and trans (**7**) *seco*ergoline derivatives (Table 3). H-

Table 2. Comparison of IC_{50} Values of *Seco*ergoline Derivatives **8**, **9**, and **11** Obtained for Inhibition of [^{3}H]GABA and [^{3}H]DASP Transport Processes, in the Presence and Absence (control) of NNC-711 and TBOA, Respectively, in Cerebrocortical Membrane Suspensions at 30 °C. Number of Experiments: $N = 2$ to $N = 6$

	IC_{50} for [^{3}H]GABA transport			IC_{50} for [^{3}H]DASP transport		
		NNC-711[a]			TBOA[a]	
compound	control	phase 1	phase 2	control	phase 1	phase 2
8	270 ± 43 μM	180 ± 7 nM	380 ± 13 μM	420 ± 57 μM	34 ± 2 nM	385 ± 16 μM
9	680 ± 87 μM	3.7 ± 0.6 nM	360 ± 8 μM	660 ± 61 μM	9.0 ± 0.2 nM	591 ± 24 μM
11	1100 ± 128 μM	44 ± 2 nM	491 ± 14 μM	1100 ± 105 μM	11.0 ± 0.9 nM	1019 ± 81 μM

[a] 100 μM each.

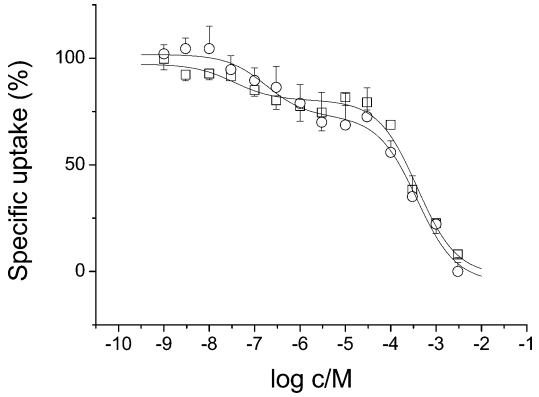

Figure 1. Comparison of inhibitory effects of **8** on [^{3}H]GABA and [^{3}H]DASP transport through cerebrocortical membranes at 30 °C in the presence of 100 μM NNC-711 and 100 μM TBOA, respectively. Symbols: ○, [^{3}H]GABA uptake; □, [^{3}H]-DASP uptake. $N = 3$.

Bonding interactions summarized in Table 3 indicated that GABA and tiagabine interacted with all the three amino acids identified by guvacine. Enantioselectivity of binding could also be observed on the basis of the number of H-bonding interactions (Table 3). All the three residues interacted with the more potent enantiomer, (*R*)nipecotic acid (IC_{50}=5.9 ± 0.8 μM[26]). In contrast, the less active enantiomer, (*S*)nipecotic acid (IC_{50}=116 ± 8 μM[26]), was found to bind to Tyr-140 and Asn-137 only (Table 3, Figure 2A,B). Using the one-TM model, however, neither binding nor cis−trans selectivity of *seco*ergoline derivatives observed in GABA transport inhibition could be predicted (Table 3).

The Two-TM Model. To understand structural requirements for transport inhibitors better, a two-TM model has been developed by adding GAT1 TM2 region to GAT1 TM3 and facing polar sides of helices against each other. In this way, H-bonding interactions of TM2 Thr-89 with GABA transport inhibitors could also be disclosed (Table 4). All compounds that were successfully docked in the one-TM model could also be docked in the two-TM model (Table 4), suggesting that TM3 residues Tyr-140, Asn-137, Ser-133 and the TM2 residue Thr-89 form a binding-crevice for GABA transport inhibitors. Moreover, (*S*)nipecotic acid and *seco*ergoline derivative with the cis (**8**), but not with the trans (**7**), configuration of ester groups was also found to bind in the binding-crevice of the two-TM model (Table 4, Figure 2C,D).

Discussion

Three of twelve *seco*ergoline derivatives (**8**, **9**, and **11**) inhibited both GABA and Glu transport processes (IC_{50} = 270−1100 μM), whereas neither these, nor the rest of *seco*ergoline derivatives, showed significant binding to $GABA_A$, $GABA_B$, AMPA, NMDA, and kainate receptors. Ineffectiveness of *seco*ergolines **2** (a guvacine derivative) and **1**, **3**, **4** (nipecotic acid derivatives) on GABA transport suggests that carboxylic substitution in the para position abolishes the inhibitory property of the compounds. Moreover, the inhibitory effect emerges by moving the carboxylic group from para (**2**) to ortho position (**9**). Among the open *seco*ergoline derivatives (**7**, **8**, **11**, and **12**), structures with the *E* configuration (**7** and **12**) did not show remarkable effects.

Although GABA and Glu transporters belong to different family and there is no homology between them,[27] all of *seco*ergoline derivatives investigated showed similar effectiveness on both transport processes. This unusual lack of selectivity among structurally different transporters with different functions can be explained by various reasons. As all the three compounds contain not only a GABA, but also a Glu bioisosteric sequence, they could act on different transporters, however, in different orientation, which may not allow similar activities on both systems. Another explanation can be the existence of a novel transporter type in cerebrocortical membrane that is able to transport both GABA and Glu (GABA-Glu transporter). In

Table 3. Molecular Mechanics Calculation of Putative H-Bonding Interactions between Transport Inhibitors and Amino Acid Residues of GAT1 TM3 (Tyr-140, Asn-137, Ser-133): The One-TM Model. Distances (Å) Were Determined between Atoms Highlighted in Bold. H-Bonding Interaction Was Accepted If Donor−Acceptor and Hydrogen−Acceptor Distances Were below 3.0 Å and 2.5 Å, Respectively (in italic)

	ligands (IC_{50} (μM))						
GAT1 TM3	GABA (5 ± 1[a])	guvacine (14 ± 3[a])	(*R*)nipecotic acid (5.9 ± 0.8[a])	(*S*)nipecotic acid (116 ± 8[a])	tiagabine (0.07 ± 0.01[a])	**7**[c] (>1000[b])	**8**[c] (270[b])
Tyr-140(**O**H)−ligand(C=**O**)	*2.60*	*2.65*	*2.63*	*2.78*	*2.50*	*2.67*	3.17
Tyr-140(O**H**)−ligand(C=**O**)	*1.79*	*1.87*	*1.97*	*2.45*	*1.71*	*1.73*	*2.43*
Asn-137(C=**O**)−ligand(CO**O**H)	*2.50*	*2.79*	*2.69*	*2.73*	*2.52*	-	-
Asn137(C=**O**)−ligand(COO**H**)	*1.62*	*1.91*	*1.90*	*2.21*	*2.13*	-	-
Ser-133(**O**H)−ligand(**N**)	*2.75*	*2.77*	*2.86*	4.96	*2.88*	5.05	*2.61*
Ser-133(O**H**)−ligand(**N**)	*2.12*	*1.85*	*1.94*	4.14	*2.12*	4.52	*2.18*

[a] Reference 26. [b] Present work. [c] Data are presented for racemic conformation with the stronger H-bonding interactions (values for the other enantiomeric conformation were within ±0.15 Å).

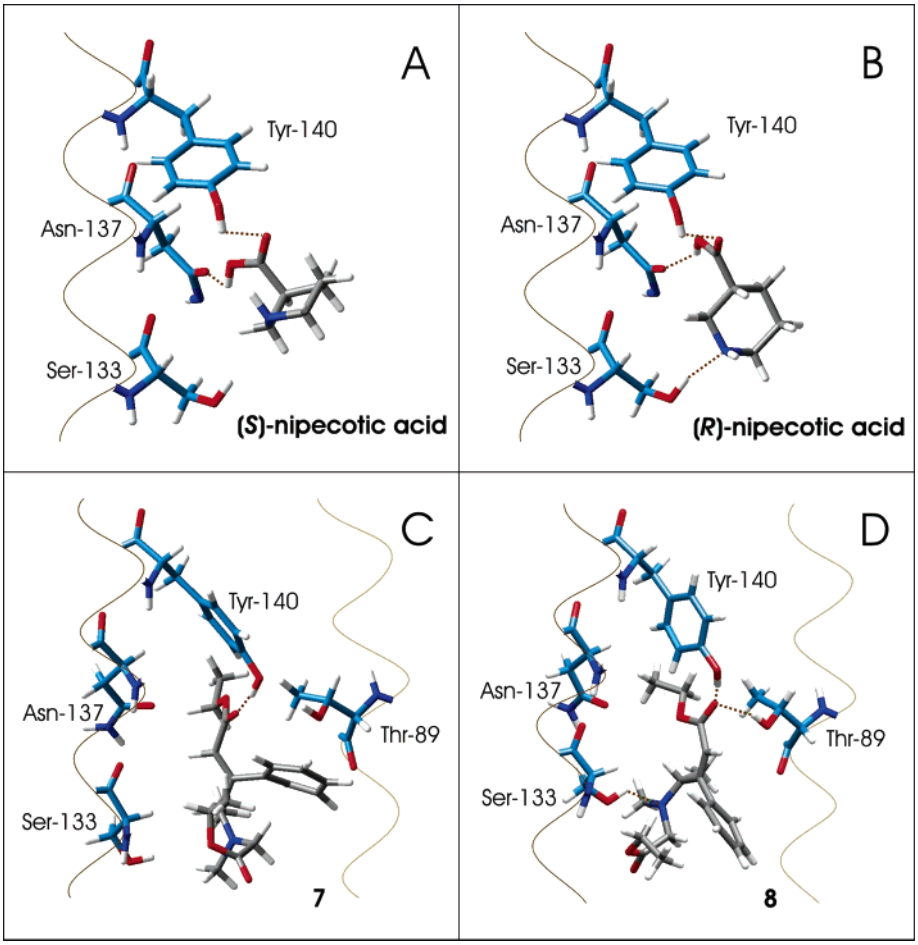

Figure 2. Different models for the 3D pharmacophore of GABA transporter type GAT1. The one-TM model: (*S*)nipecotic acid (A) and (*R*)nipecotic acid (B) were docked in GAT1 TM3. The two-TM model: *seco*ergoline derivatives **7** (C) and **8** (D) were docked in GAT1 TM2 coupled GAT1 TM3. Transmembrane α-helices are visualized as traces. Ligands (grey), and amino acid residues involved in ligand binding (light blue) are shown in stick. Nitrogen and oxygen atoms are colored blue and red, respectively. H-bonding interactions are represented by dotted lines.

Table 4. Molecular Mechanics Calculation of Putative H-Bonding Interactions between Transport Inhibitors and Amino Acid Residues of GAT1 TM3 (Tyr-140, Asn-137, Ser-133) and GAT1 TM2 (Thr-89): The Two-TM Model. Distances (Å) Were Determined between Atoms Highlighted in Bold. H-Bonding Interaction Was Accepted If Donor−Acceptor and Hydrogen−Acceptor Distances Were below 3.0 Å and 2.5 Å, Respectively (in italic)

	ligands (IC_{50} (μM))						
GAT1 TM3, GAT1 TM2	GABA (5 ± 1^a)	guvacine (14 ± 3^a)	(*R*)nipecotic acid (5.9 ± 0.8^a)	(*S*)nipecotic acid (116 ± 8^a)	tiagabine (0.07 ± 0.01^a)	**7**[c] ($>1000^b$)	**8**[c] (270^b)
Tyr-140(**O**H)−ligand(C=**O**)	*2.73*	*2.59*	*2.78*	*2.66*	*2.76*	*2.61*	*2.68*
Tyr-140(O**H**)−ligand(C=**O**)	*1.83*	*1.68*	*1.88*	*1.77*	*1.87*	*1.67*	*1.75*
Asn-137(C=**O**)−ligand(CO**O**H)	*2.64*	*2.56*	*2.60*	*2.66*	*2.72*	-	-
Asn-137(C=**O**)−ligand(COO**H**)	*1.80*	*1.68*	*1.95*	*1.83*	*1.78*	-	-
Ser-133(**O**H)−ligand(**N**)	*2.88*	*2.90*	*2.74*	*2.97*	*2.92*	4.56	*2.84*
Ser-133(O**H**)−ligand(**N**)	*2.15*	*2.26*	*2.00*	*2.10*	*2.14*	3.61	*2.20*
Thr-89(**O**H)−ligand(C=**O**)	*2.88*	*2.66*	*2.56*	*2.95*	*2.68*	3.60	*2.68*
Thr-89(O**H**)−ligand(C=**O**)	*1.97*	*1.76*	*2.14*	*2.49*	*1.79*	2.99	*1.93*

[a] Reference 26. [b] Present work. [c] Data are presented for racemic conformation with the stronger H-bonding interactions (values for the other enantiomeric conformation were within ± 0.2 Å).

this respect, it is to note that transport rates of both GABA- and Glu-containing synaptic vesicles were modulated with the same endogenous protein.[28] The existence of this protein might substantiate a proposal that both GABA and Glu transport processes can be regulated with the same compound. Furthermore, underlying mechanisms, that is inhibition on both GABA and Glu transporters vs inhibition on GABA-Glu transporter can operate in the same time. It follows that *seco*ergoline derivatives could manifest higher inhibitory potential for an isolated GABA-Glu transporter. The pharmacological approach to the isolation of the transport process mediated by a possible GABA-Glu transporter, by blocking the major GABA and Glu transport processes with high-affinity, nontransportable inhibitors, separated high- and low-capacity GABA and Glu transport processes. The high-capacity processes can correspond to transports driven by known GABA and Glu transporters. Since NNC-711 is a specific inhibitor of GAT1 (IC_{50} values were found to be 0.04, 171, 1700, and 622

μM for the cloned GAT1, GAT2, GAT3, and BGT1, respectively[24]), inhibitory effects of *seco*ergoline derivatives on both high- and low-capacity GABA transport through cerebrocortical membranes were neither expected nor found to be the same in the presence and absence of NNC-711. In contrast, inhibitory effects of **8**, **9**, and **11** on the high-capacity Glu transport process were similar to those obtained in the absence of DL-TBOA, a nearly equipotent inhibitor of Glu transporters (IC_{50} values are 70, 6, 6, 4.4, and 3.2 μM for the cloned Glu transporter types 1−5, respectively[25]), suggesting that DL-TBOA affects less the transport properties of *seco*ergoline derivatives than NNC-711 does. The low-capacity processes disclosed are unique as to *seco*ergoline derivatives **8**, **9**, and **11** inhibit them similarly, with substantially higher inhibitory potential and selectivity. The low- and the high-capacity GABA and Glu transport processes are also distinguishable on the basis of different order of inhibitory potential of **8**, **9**, and **11**. Inhibitory sequences, in order of decreasing inhibition, were **9** ≥ **11** > **8** and **8** ≥ **9** > **11**, respectively. As the inhibitory potential of compounds for the low-capacity GABA and Glu transport phases is much higher than that of any known GABA and Glu uptake inhibitors, these low-capacity processes are unlikely to be mediated by the known GABA- and Glu transporters. Indeed, such a high affinity may only be functional when the signaling amount of neurotransmitters had already been taken up by the known high-capacity processes. This way, we may conjecture the existence of a novel type of transport process characterized by extreme high affinity and low capacity with a role in some, rather general clearance mechanism in or outside the synaptic cleft. Moreover, it is hardly probable that two different targets could be affected with the same compounds in the 3−200 nM concentration range; thus, we suppose that the novel type of transport process described here may be mediated by a single target, a GABA-Glu transporter. Conclusively these findings suggest that molecules, such as *seco*ergoline derivatives **8**, **9**, and **11**, which have structural motifs allowing them to interact with both GABA and Glu transporters, do highlight the possible existence of a previously unrecognized GABA-Glu transporter.

On the basis of mutagenesis studies, Kanner and coworkers identified Tyr-140 residue in TM3 helix of GAT1, which is likely involved in ligand binding.[13] Results of GAT1 mutagenesis studies corroborate the "alternate access" model of secondary transport viewed as the alternating outward and inward reorientation of the loaded and empty binding site.[29] Thus, the minimal functional unit for Na^+ ion-coupled GABA translocation can be viewed as the third transmembrane helix (TM3) of GAT1. Thus, in the absence of the three-dimensional structure of GABA transporters the TM3 region was addressed first. On the basis of computer-aided modeling of interactions between guvacine and the GAT1 TM3 region, two additional amino acid residues have been identified, which could possibly be involved in ligand binding, Asn-137 and Ser-133. Binding interaction between the amino acid residues, Tyr-140, Asn-137, and Ser-133 and the GABA uptake inhibitors may provide a minimal model for a 3D pharmacophore of the GABA transporter. This one-TM model predicts enantioselectivity of GABA transport inhibitors. However, even the most active *seco*ergoline derivative tested cannot be docked into the binding core formed by all the three amino acids involved in the one-TM model, suggesting that more binding interactions are required to dock low-potency compounds. Indeed, the proposed model of the 3D binding-crevice involving both GAT1 TM3 and TM2 helices is able to predict cis−trans selectivity of *seco*-ergoline derivatives. Moreover, the two-TM model combined with the one-TM model can be used to estimate inhibitory potency as high- and low-potency compounds can be docked to the two-TM model, but only compounds with high affinity can fit in the one-TM model. Based on knowledge of the role of GABA-mediated inhibitory neurotransmission in the pathogenesis of several types of epilepsy, the proposed 3D pharmacophore model may provide new insights into the structural prerequisites for the anticonvulsant activity of GABA transport inhibitors.

Experimental Section

Chemistry. All compounds prepared and investigated are racemates. Melting points are uncorrected. Mass spectra were run on an AEI-MS-902 (70 eV; direct insertion) mass spectrometer. IR spectra were taken on a Nicolet 205 and Nicolet 7795 FT-IR spectrophotometers. NMR spectroscopy measurements were carried out on a Varian Unity Inova (400 MHz) instrument. Chemical shifts are given relative to TMS = 0.00 ppm. Elemental analyses (C, H, N) were carried out by Vario EL III (Elementar Analyzen Systeme GmbH) automatic microanalyzer, ionic halide content was measured by titration with mercuric perchlorate. For thin-layer chromatography (TLC) analyses MN Polygram SIL G/UV_{254} sheets were used. Preparative separations were performed by column chromatography on Merck Kieselgel 60 (0.063−0.200).

Glassware was flame dried before use. Solvents were carefully dried and purified by appropriate methods. The majority of the reactions were carried out under argon protection.

1-Methyl-2-oxo-2-phenylethylammonium chloride (**i**), diethyl 2-[(1-methyl-2-oxo-2-phenylethylamino)methylene]succinate (**ii**), diethyl 2-[methyl-(1-methyl-2-oxo-2-phenylethylamino)methyl]-succinate (**iii**), diethyl 5β-hydroxy-1,6-dimethyl-5α-phenyl-piperidine-3α,4β-dicarboxylate (**1**, **iv**, and **v**), and diethyl 1,6-dimethyl-5-phenyl-1,2,3,6-tetrahydropyridine-3,4-dicarboxylate (**2**) were prepared as described.[17]

Ethyl 1,6-Dimethyl-5β-hydroxy-5α-phenyl-3α-carboxypiperidine-4β-carboxylate (3) and 1,6-Dimethyl-5β-hydroxy-5α-phenylpipereidine-3α,4β-dicarboxylic Acid (4). To the solution of diastereomeric mixture of hydroxy-diester **1** (900 mg; 2.57 mmol) in ethanol (50 mL) was added a solution of KOH (1.6 g; 28.8 mmol) in distilled water (30 mL). The mixture was stirred at 60−70 °C for 3 h, cooled, and acidified with 1:1 aq HCl (pH 3) and evaporated in vacuo. The residue containing **3** and **4** was separated by column chromatography (eluent: ethanol−25% NH_4OH 5:1) to afford monocarboxylic acid **3** (550 mg; 66%; R_f: 0.7) and dicarboxylic acid **4** (214 mg, 28%, R_f: 0.2). **3:** pale tan crystals; mp 199−210 °C. IR (KBr): 1607 (CO_2^-); 1725 (C=O); 3140 cm^{-1} (OH). ^1H NMR (diastereomers; 400 MHz; DMSO-d_6): 0.55+0.70 (3H; 2 × t; J = 7.1 Hz; CH_2CH_3); 0.66+0.74 (3H; 2 × d; J = 6.8 Hz; 6-CH_3); 2.36+2.38 (3H; 2 × s; NCH_3); 2.50+2.86+2.54+3.25 (2H; m; H2); 2.64+2.76 (1H; 2 × q; J = 7.1 Hz; H6); 2.98+3.41 (1H; 2 × d; J = 11.6 Hz; H4); 3.20−3.30 (1H; m; H3); 3.52+3.66+3.76 (2H; 3 × q; J = 7.1 Hz; OCH_2); 4.66 (1H; brs; OH); 7.21 (1H; m; H4′); 7.24 (2H; m; H3′+H5′); 7.41+7.60 (2 × 1H; m; H2′+H6′). ^{13}C NMR (100.6 MHz; DMSO-d_6): 5.7+12.9 (6-CH_3); 13.7+13.9 (CH_2CH_3); 41.0+41.4 (C3); 42.4+42.5 (NCH_3); 44.6+54.1 (C4); 47.6+57.2 (C2); 59.3+59.7 (OCH_2); 65.7+66.1 (C6); 75.9+76.2 (C5); 125.9+126.9+127.4+127.7+128.0 (C2′+C3′+C4′+C5′+C6′); 142.5+144.1 (C1′); 171.4+172.0 (CO_2-

Et); 174.0+174.2 (CO_2H). Anal. ($C_{17}H_{23}NO_5$) C, H, N. **4:** pale tan crystals; mp 229−231 °C. IR (KBr): 1600 (CO_2^-); 3120 cm^{-1} (OH). ^1H NMR (diastereomers; 400 MHz; DMSO-d_6): 0.93+1.00 (3H; 2 × d; J = 6.8 Hz; 6-CH_3); 2.78+2.84 (3H; 2 × s; NCH_3); 2.96+3.22 (1H; 2 × d; J = 11.4 Hz; H4); 3.28 (1H; m; H3); 3.24+3.31+3.58 (2H; m; H2); 3.39+3.62 (1H; 2 × q; J = 6.8 Hz; H6); 7.25 (1H; m; H4′); 7.34 (2H; m; H3′+H5′); 7.36+7.47 (2 × 1H; 2 × m; H2′+H6′). ^{13}C NMR (100.6 MHz; DMSO-d_6): 6.1+10.8 (6-CH_3); 40.9+41.5 (C3); 43.4+44.1 (NCH_3); 45.7+55.5 (C4); 48.1+56.2 (C2); 65.5+66.2 (C6); 75.3+75.3 (C5); 125.5+126.6+128.2+128.8+129.0 (C2′+C3′+C4′+C5′+C6′); 141.3+ 141.7 (C1′); 176.1+176.6+177.8+178.6 (2 × CO_2H). Anal. ($C_{15}H_{19}NO_5$) C, H, N.

Ethyl (1-Methyl-2-oxo-2-phenylethylamino)acetate Hydrochloride (5). To the suspension of amine HCl (**i**) (9.25 g; 50 mmol) in THF (100 mL) was added triethylamine (13.9 mL; 10.1 g; 100 mmol), and the mixture was cooled in ice bath to 0 °C. Into the stirred mixture was dropped in small portions ethyl bromoacetate (5.5 mL; 8.35 g; 50 mmol) over 30 min. The mixture was then stirred at ambient temperature for 1−1.5 h, and progress of the alkylation could be followed by TLC (hexane−EtOAc 1:1 after treating the sheet with NH_3 vapor; R_f **5** > R_f **i**). Triethylammonium chloride precipitated was filtered off and the solution evaporated in vacuo. The residue was purified by column chromatography (eluent: chloroform−acetonitrile 4:1) to afford the alkylated base as an oil (7.05 g; 60%). The compound was isolated and characterized as hydrochloride salt **5** (prepared in EtOAc) as off-white crystals (7.0 g; 52%), mp 131−133 °C (ethyl acetate). IR (KBr): 1680 (C=O ketone); 1755 (C=O ester); 3410 cm^{-1} ($^+NH_2$). ^1H NMR (base; 400 MHz; $CDCl_3$): 1.23 (3H; t; CH_2CH_3); 1.38 (3H; d; J = 6.9 Hz; CH_3CHN); 2.20 (1H; brs; NH); 3.35+3.45 (2 × 1H; 2 × d; J_{gem} = 16.5 Hz; NCH_2CO); 4.18 (2H; q; OCH_2); 4.41 (1H; q; J = 6.9 Hz; CH_3CHN); 7.49 (2H; t; H3′+H5′); 7.61 (1H; t; H4′); 7.98 (2H; d; H2′+H6′), Anal. ($C_{13}H_{18}ClNO_3$) C, H, N, Cl.

Methyl (1-Methyl-2-oxo-2-phenylethylamino)acetate Hydrochloride (vi). The methyl ester analogue of **5** (**vi**) was prepared similarly to the previous procedure. Amine HCl **i** (3.7 g; 20 mmol) was alkylated with methyl bromoacetate to afford the target molecule after chromatography as a pale yellow oil (2.5 g; 57%). The compound was isolated and characterized as hydrochloride salt **vi** (prepared in chloroform) as off-white crystals (2.5 g; 48%), mp 156−158 °C (methanol−diethyl ether). IR (KBr): 1680 (C=O ketone); 1740 (C=O ester); 3420 cm^{-1} ($^+NH_2$). ^1H NMR (400 MHz; $CDCl_3$+DMSO-d_6): 1.64 (3H; d; J = 7.0 Hz; CH_3CHN); 3.83 (3H; s; OCH_3); 4.01+4.09 (2 × 1H; 2 × d; J_{gem} = 16.5 Hz; $^+NCH_2CO$); 5.39 (1H; q; J = 7.0 Hz; CH_3CHN^+); 7.58 (2H; t; H3′+H5′); 7.71 (1H; t; H4′); 8.03 (2H; d; H2′+H6′); 10.10 (2H; brs; $^+NH_2$). Anal. ($C_{12}H_{16}ClNO_3$) C, H, N, Cl.

Ethyl [Methyl-(1-methyl-2-oxo-2-phenylethyl)amino]-acetate Hydrochloride (6). The HCl salt **5** (6.8 g; 25 mmol) was transformed into the corresponding base (oil) and its solution in dry acetonitrile (400 mL) and acetic acid (95 mL) was cooled to 0 °C. Into the stirred solution, sodium cyanoborohydride (6.1 g; 96 mmol) and 36% aq formaldehyde solution (140 mL; 1.66 mol) was added. The mixture was stirred at 0 °C, progress of the methylation could be followed by TLC (hexanes−EtOAc 1:1 after treating the sheet with NH_3 vapor; R_f **6**>R_f **5**). The reaction was complete after 30−40 min. The mixture was diluted with water (500 mL), its pH was adjusted to neutral with Na_2CO_3 solution and extracted with chloroform (3 × 300 mL). The combined organic phase was dried (Na_2SO_4) and evaporated. The residue was dissolved in ethanol-diethyl ether 1:5 (50 mL), and acidified with 2N HCl/dioxane (pH 2) to give white crystals of target compound **6** (6.35 g; 89%). Mp 155−157 °C (acetone). IR (KBr): 1680 (C=O ketone); 1738 (C=O ester); 3400 cm^{-1} ($^+NH_2$). ^1H NMR (400 MHz; DMSO-d_6): 1.25 (3H; t; CH_2CH_3); 1.50 (3H; d; J = 6.8 Hz; CH_3CHN) 2.89 (3H; s NCH_3); 4.08+4.11 (2 × 1H; 2 × d; J_{gem} = 16.8 Hz; $^+NCH_2CO$); 4.22 (2H; q; OCH_2); 5.35 (1H; q; J = 6.8 Hz; CH_3CHN); 7.59 (2H; t; H3′+H5′); 7.70 (1H; t; H4′); 8.03 (2H; d; H2′+H6′); 10.20 (1H; brs; ^+NH). Anal. ($C_{14}H_{20}ClNO_3$) C, H, N, Cl.

Methyl [Methyl-(1-methyl-2-oxo-2-phenylethyl)amino]-acetate Hydrochloride (10). Alkylated amine HCl **vi** (1.6 g; 6.2 mmol) was methylated into the methyl ester analogue of **6** (**10**) similarly to the previous procedure to afford the target molecule, which was isolated as oily HCl salt (1.68 g; quantitative yield) IR (KBr): 1680 (C=O ketone); 1740 (C=O ester); 3410 cm^{-1} ($^+NH_2$). ^1H NMR (base; 400 MHz; $CDCl_3$): 1.31 (3H; d; J = 6.8 Hz; CH_3CHN); 2.45 (3H; s; NCH_3); 3.50+3.58 (2 × 1H; 2 × d; J_{gem} = 16.9 Hz; NCH_2CO); 3.70 (3H; s; OCH_3); 4.53 (1H; q; J = 6.8 Hz; CH_3CHN); 7.44 (2H; t; H3′+H5′); 7.58 (1H; t; H4′); 8.06 (2H; d H2′+H6′). Anal. ($C_{13}H_{18}ClNO_3$) C, H, N, Cl.

Ethyl 4-[(Ethoxycarbonylmethyl)methylamino]-3-hydroxy-3-phenylpentanoate (vii). A well-dried three-neck flask was immersed in an acetone/dry CO_2 cooling bath (−78 °C), and under argon protection, 1 N lithium bis(trimethylsilyl)amide/THF solution (6 mL; 6 mmol) and ethyl acetate (0.60 mL; 0.54 g; 6 mmol) were admixed. The solution was stirred for 15 min at −78 °C. Then a solution of aminoketone in dry THF (40 mL), obtained from the solution of the HCl salt (**6**) (570 mg; 2 mmol) in water (10 mL) by having treated with 10% aq solution of $NaHCO_3$ (pH 7), extracted with chloroform, and evaporated, was admixed at −78 °C. Progress of the addition could be followed by TLC (hexane−ethyl acetate 4:1; R_f **vii**> R_f **6**). The reaction was usually complete after 1 h. At this temperature 20% aq HCl (0.4 mL; ∼2.4 mmol) was added to the mixture, which was left to warm to room temperature. The pH of the mixture was adjusted to 7 when needed. After distilling off THF in vacuo, the residue was dissolved in a mixture of chloroform (50 mL) and water (30 mL). The organic phase was dried (Na_2SO_4) and evaporated and the residue purified by column chromatography (eluent: hexane−ethyl acetate 9:1). After evaporation to dryness the inseparable diastereomeric mixture of hydroxy-diesters (**vii**) was obtained as a pale yellow oily base (500 mg; 75%). As the compound proved to be rather unstable, it was used in the next step immediately. IR (KBr): 1730 (broad; C=O ester); 3460 cm^{-1} (OH). ^1H NMR (400 MHz; $CDCl_3$): 1.00 (3H; d; J = 6.8 Hz; CH_3CHN); 1.05+1.26 (2 × 3H; 2 × t; 2 × CH_2CH_3); 2.20 (3H; s; NCH_3); 2.86+3.44 (2 × 1H; 2 × d; NCH_2CO); 2.93 (1H; q; J = 6.8 Hz; CH_3CHN); 3.06+3.11 (2 × 1H; 2 × d; J_{gem}=16.7 Hz; CCH_2CO); 4.00+4.18 (2 × 2H; 2 × q; 2 × OCH_2); 7.20−7.50 (5H; m; aromatic protons).

Methyl 4-[(Methoxycarbonylmethyl)methylamino]-3-hydroxy-3-phenylpentanoate (viii). The dimethyl ester analogue of **vii** (**viii**) was prepared from amine **10** similarly to the previous procedure; instead of ethyl acetate, an equivalent amount of methyl acetate was used in the reaction. In a 2 mmol charge after purification with column chromatography (eluent: hexane−ethyl acetate 9:1) the inseparable diastereomeric mixture of hydroxy-diesters (**viii**) was obtained as a pale yellow oily base (409 mg; 66%). As the compound proved to be rather unstable, it was used in the next step immediately. IR (KBr): 1730 (broad; C=O ester); 3450 cm^{-1} (OH). ^1H NMR (400 MHz; $CDCl_3$): 1.01 (3H; d; J = 7.0 Hz; CH_3CHN); 2.21 (3H; s; NCH_3); 2.89+3.43 (2 × 1H; 2 × d; J_{gem}= 16 Hz; NCH_2CO); 2.94 (1H; q; J = 7.0 Hz; CH_3CHN); 3.11+3.13 (2 × 1H; 2 × d; J_{gem}= 16.7 Hz; CCH_2CO); 3.55+3.67 (2 × 3H; 2 × s; 2 × OCH_3); 3.65 (1H; brs; OH); 7.23 (1H; m; H4′); 7.28 (2H; m; H3′+H5′); 7.46 (2H; m; H2′+H6′).

***E* and *Z* Ethyl 4-[(Ethoxycarbonylmethyl)methylamino]-2-methyl-3-phenylpent-2-enoate (7 and 8). Method A** (via phosphonate condensation of ketone **6**). In a two-necked flask 50% NaH dispersion in mineral oil (1.8 g; 36 mmol) was washed with dry THF (2 × 25 mL) until oil-free. Then it was suspended in dry THF (20 mL) and cooled to 0−5 °C, and a solution of triethyl phosphonoacetate (6.72 g; 30 mmol) in dry THF (10 mL) was added. After stirring the mixture at 0−5 °C for 30 min, the temperature was allowed to warm to room temperature, and a suspension of ketone HCl **6** (1.14 g; 4 mmol) in dry THF (20 mL) was admixed. The progress of the condensation followed by TLC (hexane−ethyl acetate 4:1; R_f

7 and **8** > R_f **6**). The reaction usually was complete (over 90% conversion) after 3 days. Then water (100 mL) was added, the THF was distilled off in reduced pressure, and the water phase was extracted with chloroform (3 × 50 mL). The combined organic phase was dried and evaporated in vacuo, and the residue was separated by column chromatography (eluent: hexane−ethyl acetate 9:1). The first compound eluted from the column proved to be the *Z* geometric isomer **8** (310 mg; 25%). IR (KBr): 1690 (C=O conjug ester); 1735 cm^{-1} (C=O ester). ^1H NMR (400 MHz; $CDCl_3$): 1.20 (3H; d; J = 7.0 Hz; CH_3-CHN); 1.27+1.32 (2 × 3H; 2 × t; 2 × CH_2CH_3); 2.43 (3H; s; NCH_3); 3.27+3.52 (2 × 1H; 2 × d; J_{gem}=16.2 Hz; NCH_2CO); 4.16+4.21 (2 × 2H; 2 × q; 2 × OCH_2); 4.78 (1H; q; J = 7.0 Hz; CH_3CHN); 5.98 (1H; s; =CH); 7.31−7.35 (3 × 1H; m; H3′+H4′+H5′); 7.67 (2H; m; H2′+H6′). NOE: 5.98 (=CH) → 7.67 (H2′+H6′). Anal. ($C_{18}H_{25}NO_4$) C, H, N. The second compound eluted from the column proved to be the *E* geometric isomer **7** (330 mg; 26%). IR (KBr): 1700 (C=O conjug ester); 1735 cm^{-1} (C=O ester). ^1H NMR (base; 400 MHz; $CDCl_3$): 1.05+1.27 (2 × 3H; 2 × t; 2 × CH_2CH_3); 1.15 (3H; d; J = 6.8 Hz; CH_3CHN); 2.47 (3H; s; NCH_3); 3.38+3.49 (2 × 1H; 2 × d; J_{gem}=16.6 Hz; NCH_2CO); 3.60 (1H; q; J = 6.8 Hz; CH_3CHN); 3.98+4.16 (2 × 2H; 2 × q; 2 × OCH_2); 6.19 (1H; d; J = 1.5 Hz; =CH); 7.17 (2H; m; H2′+H3′); 7.33 (3 × 1H; m; H3′+ H4′+H5′). NOE: 6.19 (=CH) → 1.15+3.60 (CH_3CHN); 2.47 (N−CH_3). Anal. ($C_{18}H_{25}NO_4$) C, H, N. In binding and uptake measurements the HCl salts of both isomers were investigated. **Method B** (via water elimination from **vii**). To the solution of the oily hydroxydiester **vii** (675 mg; 2 mmol) in pyridine (20 mL) was added $POCl_3$ (0.6 mL; 6.5 mmol), and the mixture was refluxed on a 120 °C oil bath. Progress of the water elimination could be followed by TLC (chloroform−acetonitrile 9:1; R_f **7** and **8** > R_f **vii**). The conversion was usually complete after 2−3 h. The mixture was cooled and evaporated in vacuo, and the residue was dissolved in a mixture of chloroform (50 mL) and water (20 mL), while the pH of the water phase was adjusted to a value of 7−7.5. The organic phase was dried (Na_2SO_4) and evaporated, and the residue was purified by column chromatography (eluent: chloroform−acetonitrile 15:1 or hexane−ethyl acetate 9:1). In this way mainly *Z* geometric isomer **8** is obtained (290 mg; 45%) along with some isomer *E* (**7**) as minor product (45 mg; 7%). Both isomers obtained in this way proved to be identical (TLC, NMR) with those prepared according to Method A.

***Z* and *E* Methyl 4-[(Methoxycarbonylmethyl)methylamino)-2-methyl-3-phenylpent-2-enoate (11 and 12).** The two geometric isomers **11** and **12** were prepared in analogous way described in the previous example by both methods and were characterized as oily hydrochloride salts. **11** HCl salt: oil; yield after chromatography: 30%. IR (KBr): 1690 (C=O conjug ester); 1735 cm^{-1} (C=O ester). ^1H NMR (400 MHz; $CDCl_3$): 1.76 (3H; d; J = 6.8 Hz; CH_3CHN^+); 3.21 (3H; s; $^+N-CH_3$); 3.83+3.86 (2 × 3H; 2 × s; 2 × OCH_3); 4.25+4.46 (2 × 1H; 2 × d; J_{gem}=16.5 Hz; $^+NCH_2CO$); 5.93 (1H; q; J = 6.8 Hz; CH_3CHN^+); 6.27 (1H; s; =CH); 7.20−7.55 (3H; m; H3′+H4′+H5′); 7.68 (2H; m; H2′+H6′). NOE: 6.27 (=CH) → 7.68 (H2′+H6′). Anal. ($C_{16}H_{22}ClNO_4$) C, H, N, Cl. **12** HCl salt: oil; yield after chromatography: 30%. IR (KBr): 1690 (C=O conjug ester); 1730 cm^{-1} (C=O ester). ^1H NMR (400 MHz; $CDCl_3$):1.76 (3H; d; J = 6.9 Hz; CH_3CHN); 3.05 (3H; s; $^+N-CH_3$); 3.60+3.76 (2 × 3H; 2 × s; 2 × OCH_3); 4.02+4.06 (2 × 1H; 2 × d; J_{gem}=17.0 Hz; $^+NCH_2CO$); 4.62 (1H; q; J = 6.9 Hz; CH_3CHN^+); 7.06 (1H; s; =CH); 7.21 (2H; m; H2′+H6′); 7.30−7.45 (3H; m; H3′+H4′+H5′). NOE: 7.06 (=CH) → 1.76+4.62 (CH_3CHN); 3.05 ($^+N-CH_3$). Anal. ($C_{16}H_{22}ClNO_4$) C, H, N, Cl.

Ethyl 1,6-Dimethyl-3-oxo-5-phenyl-1,2,3,6-tetrahydropyridine-2-carboxylate (9). To the stirred suspension of hydrochloride salt of pure *Z* geometric isomer **8** (310 mg; 0.87 mmol) in dry THF (10 mL) was added 1 N lithium bis(trimethylsilyl)amide/THF solution (2 mL; 2 mmol) at ambient temperature. Progress of the Dieckmann condensation could be followed by TLC (chloroform−acetonitrile 9:1; R_f **9** > R_f **8**). After 10 h, a further amount of 1 N lithium bis(trimethylsilyl)amide/THF (3 mL; 3 mmol) was added to the stirred mixture. The reaction was usually complete after 12 h. At this temperature the mixture was neutralized with 20% aq HCl (pH7). After distilling off the THF in vacuo, the residue was dissolved in a mixture of chloroform (20 mL) and water (10 mL). The organic phase was dried (Na_2SO_4) and evaporated, and the residue was purified by column chromatography (eluent: chloroform−acetonitrile 9:1). After evaporation the pyridone **9** was isolated as an oily base (101 mg; 42%), which exists in equilibrium with chelated enol form. IR (KBr): 1640 (C=C; C=O conjug H-bridged ester); 1680 (C=O ketone); 1730 (C=O ester); 3300 cm^{-1} (chel OH). ^1H NMR (400 MHz; $CDCl_3$): 1.20 (3H; d; 2-CH_3); 1.39 (3H; t; CH_2CH_3); 2.40 (0.5 × 1H; s; H6 keto form); 2.55 (3H; s; 1-CH_3); 3.94 (1H; q; H2); 4.31 (0.5 × 2H; q; OCH_2 keto form); 4.46 (0.5 × 2H; q; OCH_2 enol form); 6.39 (1H; s; H4); 7.30−7.50 (5H; m; aromatic protons); 11.10 (0.5 × 1H; s; OH enol form). Anal. ($C_{16}H_{19}NO_3$) C, H, N. In binding and uptake measurements the HCl salt was investigated.

In Vitro Pharmacology. Three to six week old male Wistar rats purchased from Toxicoop (Budapest, Hungary) were kept and used in accordance with the European Council Directive of 24 November 1986 (86/609/EEC) and with the Hungarian Animal Act, 1998, and associated guidelines. Compounds used in the experiments: tris(hydroxymethyl)-aminomethane (TRIS) (Reanal: Budapest, Hungary); *N*-[2-hydroxyethyl]piperazine-*N*′-[2-ethanesulfonic acid] (HEPES), aprotinin, leupeptin, antipain, pepstatin A, phenyl methanesulfonyl fluoride (PMSF), butylated hydroxytoluene (BHT), t-PDC, guvacine, (1*S*,9*R*)(−)bicuculline methiodide (BMI), (±)2(2-chlorophenyl)-2-(methylamino)cyclohexanone ((±)ketamine), and L)glutamic acid (Sigma-Aldrich, Budapest, Hungary); $CaCl_2$, NaCl, KCl, $MgCl_2$, NaOH, and glucose (Fluka: Budapest, Hungary); (*S*)(−)-5-fluorowillardiine, [^{3}H](*S*)(−)5-fluorowillardiine (36 Ci/mmol), (*RS*)4-amino-3-(4-chlorophenyl)butanoic acid ((*RS*)baclofen), [^{3}H](+)MK 801 (32,75 Ci/mmol) (Tocris: Bristol, U.K.); [^{3}H]kainic acid (58 Ci/mmol) (NEN: Boston, MA); [^{3}H](D)asparatic acid ([^{3}H]DASP) (24 Ci/mmol), [^{3}H]GABA (61 Ci/mmol) (Amersham: Little Chalfont, U.K.); HiSafe 3 scintillation mixture (LKB−Wallac: Bromma, Sweden) and spectroscopic grade dimethyl sulfoxide (DMSO, Merck: Budapest, Hungary). Buffers had the following compositions: A, 145 mM NaCl, 5 mM KCl, 1 mM $CaCl_2$, 1 mM $MgCl_2$, 10 mM glucose, 0.1 mM aminooxyacetate, 2 mM $NaHCO_3$, and 20 mM HEPES adjusted to pH 7.5 with NaOH; B, 50 mM TRIS and 2.5 mM $CaCl_2$ adjusted to pH 7.4 with HCl;

GABA and Glu Transport.[21] Native plasma membrane vesicle fraction was obtained as described before with the exception that the final pellet was suspended in 15 mL of buffer A.

Receptor Binding Assays. Affinity of test compounds to $GABA_A$,[30] NMDA,[31] AMPA,[32] and kainate[31] receptors were determined as described before. IC_{50} values for standards were found to be 0.5 ± 0.1 μM (BMI on $GABA_A$ receptor), 1.6 ± 0.2 μM ((*S*)AMPA on AMPA receptor), 0.04 ± 0.01 μM (kainate on kainate receptor), and 0.51 ± 0.14 μM (ketamine on NMDA receptor). Affinity for $GABA_B$ receptor was determined according to Hill and Bowery[33] with modifications. Briefly, rats were decapitated and the brains were rapidly removed and homogenized in 15 vol of ice-cold 0.32 M sucrose solution. The homogenate was centrifuged at 1000*g* for 10 min, the pellet was discarded, and the supernatant fluid was centrifuged at 20000*g* for 20 min. The pellet was resuspended in 15 vol of distilled water, lyzed on ice for 30 min, and centrifuged at 8000*g* for 20 min. The supernatant and the "buffy coat layer" loosely attached to the pellet was collected and centrifuged at 40000*g* for 20 min. The pellet was resuspended and pelleted at 40000*g* for 20 min in 15 vol of distilled water. The pellet was frozen at −20 °C for at least 18 h. On the following day the pellet was thawed, resuspended in 10 vol of buffer B, and after incubation at 25 °C for 45 min, it was centrifuged at 7000*g* for 10 min. The pellet was resuspended in 10 vol of buffer B and centrifuged at 7000*g* for 10 min. This washing procedure was repeated one more time, and the final pellet

was resuspended in 10 vol of buffer B. Aliquots (1000 μL) of crude synaptic membrane homogenate in buffer B were incubated with a 1000 μL solution of test compounds at 20 °C for 40 min in the presence of a 200 μL solution of [^{3}H]GABA and isoguvacine in final concentration of 15 nM and 40 μM, respectively. The nonspecific binding was determined with 100 μM (*RS*)baclofen. After the incubation, samples of 1000 μL were centrifuged in Eppendorf tubes at 11000*g* for 3 min at 20 °C. The supernatant of the samples was aspirated under vacuum, and the pellets were rinsed two times with ice-cold buffer B. The pellet was solubilized with vortex in 150 μL of 10% SDS solution, and the radioactivity of samples was counted in HiSafe 3 scintillation mixture. IC_{50} of the standard, (*RS*)baclofen, was found to be 0.4 ± 0.09 μM.

Molecular Modeling. All calculations were performed using Sybyl 6.6 package (SYBYL 6.7.1 Tripos Inc., 1699 South Hanley Rd., St. Louis, Missouri, 63144) with Tripos force field and Gasteiger-Hückel charges. The Tripos force field was used throughout the calculations for its simplicity, robustness, and considerably faster execution times as compared to other, more sophisticated force fields (e.g. AMBER or MMFF94) and because of the inherent uncertainty of side chain positions in a model to be constructed on the basis of the amino acid sequence alone. The TM regions (TM3 and TM2) were built by Sybyl *Build Biopolymer* command based on amino acid sequence of TM3 (TM2) followed by minimization with simplexing and applying Powell algorithm. The relative orientation of TM3 and TM2 was calculated using a knowledge-based scale for transmembrane helix structure prediction.[34] Geometry of each ligand molecule was obtained upon molecular mechanics energy minimization of the positively charged form using simplexing and applying Powell and BFGS algorithm alternately. Docking procedures were performed as follows:[6] ligand molecules were positioned in the hypothesized manner (C=O group of COOH faced to Tyr-140 of TM3 and Thr-89 of TM2, OH group of COOH faced to Asn-137 and N faced to Ser-133). After minor manual adjustments for finding a favorable initial position for the ligand, the energy of the system was minimized throughout the docking procedure during which neither site nor ligand geometry was fixed. H-Bonding interaction was accepted if donor−acceptor and hydrogen−acceptor distances were below 3.0 Å and 2.5 Å, respectively.[35]

Data Analysis. Duplicate measurements of binding and transport were repeated in two to six experiments ($N = 2$ to $N = 6$). Data are expressed as means ± SD and were analyzed using one-way analysis of variances (ANOVAs, Origin ver. 6.1). A value of $P < 0.05$ was considered significant. Concentration-inhibition curves were fitted with the use of Origin ver. 6.1.

Acknowledgment. This work was supported by grants 1/047 NKFP MediChem (Hungary), OTKA T031753, Center of Excellence on Biomolecular Chemistry QLK2-CT-2002-90436 (EU), and Bolyai fellowship to Éva Szárics, Ph.D. Professor István Simon (Institute of Enzymology, Biological Research Center, Hungarian Academy of Sciences) is gratefully acknowledged for his advice on two-TM model building.

References

(1) Browne, T. R.; Holmes, G. L. Epilepsy. *New Eng. J. Med.* **2001**, *344*, 1145−1151.
(2) Treiman, D. M. GABAergic mechanisms in epilepsy. *Epilepsia* **2001**, *42*, 8−12.
(3) Kwan, P.; Sills, G. J.; Brodie, M. J. The mechanisms of action of commonly used antiepileptic drugs. *Pharmacol. Ther.* **2001**, *90*, 21−34.
(4) Löscher, W. New visions in the pharmacology of anticonvulsion. *Eur. J. Pharmacol.* **1998**, *342*, 1−13.
(5) Lasztóczi, B.; Kovács, R.; Nyikos, L.; Kardos, J. A glutamate receptor subtype antagonist inhibits seizures in rat hippocampal slices. *Neuroreport* **2002**, *13*, 351−356.
(6) Szárics, É.; Nyikos, L.; Barabás, P.; Kovács, I.; Skuban, N.; Temesváriné-Major, E.; Egyed, O.; Nagy, P. I.; Kökösi, J.; Takács-Novák, K.; Kardos, J. Quinazolone-alkyl-carboxylic acid derivatives inhibit transmembrane Ca^{2+} ion flux to (+)[*S*]-α-amino-3-hydroxy-5-methylisoxazole-4-propionic acid. *Mol. Pharmacol.* **2001**, *59*, 920−928.
(7) Löscher, W. Current status and future directions in the pharmacotherapy of epilepsy. *Trends Pharmacol. Sci.* **2002**, *23*, 113−118.
(8) Dalby, N. O. GABA-level increasing and anticonvulsant effects of three different GABA uptake inhibitors. *Neuropharmacol.* **2000**, *39*, 2399−2407.
(9) Frølund, B.; Ebert, B.; Kristiansen, U.; Liljefors, T.; Krogsgaard-Larsen, P. $GABA_A$ receptor ligands and their therapeutic potential. *Curr. Topics Med. Chem.* **2002**, *2*, 817−832.
(10) Cromer, B. A.; Morton, C. J.; Parker, M. W. Anxiety over $GABA_A$ receptor structure relieved by AChBP. *Trends Pharmacol. Sci.* **2002**, *27*, 280−287.
(11) Wipf, D.; Ludewig, U.; Tegeder, M.; Rentsch, D.; Koch, W.; Frommer, W. B. Conservation of amino acid transporters in fungi, plants and animals. *Trends Biol. Sci.* **2002**, *27*, 139−147.
(12) Kleinberger-Doron, N.; Kanner, B. I. Identification of Tryptophan Residues Critical for the Function and Targeting of the γ-Aminobutyric Acid Transporter (Subtype A). *J. Biol. Chem.* **1994**, *269*, 3063−3067.
(13) Bismuth, Y.; Kavanaugh, M. P.; Kanner, B. I. Tyrosine 140 of the γ-aminobutyric acid transporter GAT-1 plays a critical role in neurotransmitter recognition. *J. Biol. Chem.* **1997**, *272*, 16096−16102.
(14) Bennett, G. B.; Mason, R. B.; Alden, L. J.; Roach, J. B., Jr. Synthesis and antiinflammatory activity of trisubstituted pyrimidines and triazines. *J. Med. Chem.* **1978**, *21*, 623−628.
(15) House, H. O.; Berkowitz, W. F. The Neber rearrangement of substituted desoxybenzoin oxime tosylates. *J. Org. Chem.* **1963**, *28*, 307−311.
(16) Stoll, A.; Rutschmann, J.; Petrzilka, Th. Über Derivate des 1;3;4;5-Tetrahydro-benz[c; d]indols. *Helv. Chim. Acta* **1950**, *33*, 2257−2261.
(17) Moldvai, I.; Temesvári-Major, E.; Incze, M.; Platthy, T.; Gács-Baitz, E.; Szántay, Cs. Chemistry of indoles carrying a basic function. Part VII. A new aspect of Stobbe reaction. *Heterocycles* **2003**, *60*, 309−319.
(18) Rathke, M. W. The preparation of lithio ethyl acetate. A simple procedure for the conversion of aldehydes and ketones to β-hydroxy esters. *J. Am. Chem. Soc.* **1970**, *92*, 3222−3223.
(19) Mehta, G.; Murthy, A. N.; Sivakumar-Reddy, D.; Veere-Reddy, A. A general approach to linearly fused triquinane natural products. Total synthesis of (±)-hirsutene, (±)-corioline and (±)-capnellene. *J. Am. Chem. Soc.* **1986**, *108*, 3443−3452.
(20) Wadworth, W. S., Jr.; Emmons, W. D. The utility of phosphonate carbanions in olefin synthesis. *J. Am. Chem. Soc.* **1961**, *83*, 1733−1738.
(21) Kardos, J.; Kovács, I.; Blandl, T.; Cash, D. J. Modulation of GABA flux across rat brain membranes resolved by a rapid quenched incubation technique. *Neurosci. Lett.* **1994**, *182*, 73−76.
(22) Ali, F. E.; Bondinell, W. E.; Dandridge, P. A.; Frazee, J. S.; Garvey, E.; Girard, G. R.; Kaiser, C.; Ku, T. W.; Lafferty, J. J.; Moonsammy, G. I.; Oh, H. J.; Rush, J. A.; Setler, P. E.; Stringer, O. D.; Venlavsky, J. W.; Volpe, B. W.; Yunger, L. M.; Zirkle, C. L. Orally active and potent inhibitors of γ-aminobutyric acid uptake. *J. Med. Chem.* **1985**, *28*, 653−660.
(23) Wang, G. J.; Chung, H. J.; Schnuer, J.; Pratt, K.; Zable, A. C.; Kavanaugh, M. P.; Rosenberg, P. A. High affinity glutamate transport in rat cortical neurons in culture. *Mol. Pharmacol.* **1998**, *53*, 88−96.
(24) Borden, L. A.; Murali Dhar, T. G.; Smith, K. E.; Weinshank, R. L.; Branchek, T. A.; Gluchowski, C. Tiagabine, SK&F 89976-A, CI-966, and NNC-711 are selective for the cloned GABA transporter GAT-1. *Eur. J. Pharmacol.* **1994**, *269*, 219−224.
(25) Shimamoto, K.; Lebrun, B.; Yasuda-Kamatani, Y.; Sakaitani, M.; Shigeri, Y.; Yumoto, N.; Nakajima, T. DL-threo-beta-benzyloxyaspartate, a potent blocker of excitatory amino acid transporters. *Mol Pharmacol.* **1998**, *53*, 195−201.
(26) Dhar, T. G. M.; Borden, L. A.; Tyagarajan, S.; Smith, K. E.; Branchek, T. A.; Weinshank, R. L.; Gluchowski, C. Design, synthesis and evaluation of substituted triarylnipecotic acid derivatives as GABA uptake inhibitors: identification of a ligand with moderate affinity and selectivity for the cloned human GABA transporter GAT-3. *J. Med. Chem.* **1994**, *37*, 2334−2342.
(27) Amara, S. G. Neurotransmitter transporters: new insights into structure; function and pharmacology. *Rev. Bras. Biol.* **1996**, *56*, 5−19.
(28) Özkan, E. D.; Lee, F. S.; Ueda, T. A protein factor that inhibits ATP-dependent glutamate and γ-aminobutyric acid accumulation into synaptic vesicles: Purification and initial characterization. *Proc. Natl. Acad. Sci. U.S.A.* **1997**, *94*, 4137−4142.

(29) Veenhoff, L. M.; Heuberger, E. H. M. L.; Poolman, B. Quaternary structure and function of transport proteins. *Trends Biol. Sci.* **2002**, *27*, 242−249.
(30) Kardos, J.; Blaskó, G.; Kerekes, P.; Kovács, I.; Simonyi, M. Inhibition of [^{3}H]GABA binding to rat brain synaptic membranes by bicuculline related alkaloids. *Biochem. Pharmacol.* **1984**, *33*, 3537−3545.
(31) Kovács, I.; Lasztóczi, B.; Szárics, É.; Héja, L.; Sági, G.; Kardos, J. Characterisation of an uridine-specific binding site in rat cerebrocortical homogenates. *Neurochem. Int.* **2003**, *43*, 101−112.
(32) Kovács, I.; Simon, Á.; Szárics, É.; Barabás, P.; Héja, L.; Nyikos, L.; Kardos, J. Cyclothiazide binding to functionally active AMPA receptor reveals genuine allosteric interaction with agonist binding sites. *Neurochem. Int.* **2004**, *44*, 271−280.
(33) Hill, D. R.; Bowery, N. G. ^{3}H-baclofen and ^{3}H-GABA bind to bicuculline-insensitive $GABA_B$ sites in rat brain. *Nature* **1981**, *290*, 149−152.
(34) Pilpel, Y.; Ben-Tal, N.; Lancet, D. kPROT: A knowledge-based scale for the propensity of residue orientation in transmembrane segments. Application to membrane protein structure prediction. *J. Mol. Biol.* **1999**, *294*, 921−935.
(35) McDonald, I. K.; Thornton, J. M. Satisfying hydrogen bonding potential in proteins. *J. Mol. Biol.* **1994**, *238*, 777−793.

JM040809C